

# **Modelling of bio-inspired vision system for velocity estimation**

by

**Sreeja Rajesh**

B.E. (Electrical and Electronic, First Class Honours),  
Bharathiyar University, India, 1999

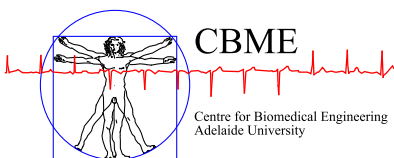
Thesis submitted for the degree of

**Doctor of Philosophy**

in

School of Electrical and Electronic Engineering,  
Faculty of Engineering, Computer and Mathematical Sciences  
University of Adelaide, Australia

November, 2007



© 2007  
Sreeja Rajesh  
All Rights Reserved



# Contents

Heading	Page
<b>Contents</b>	<b>iii</b>
<b>Abstract</b>	<b>ix</b>
<b>Statement of Originality</b>	<b>xi</b>
<b>Acknowledgments</b>	<b>xiii</b>
<b>Thesis Conventions</b>	<b>xv</b>
<b>Publications</b>	<b>xvii</b>
<b>List of Figures</b>	<b>xix</b>
<b>List of Tables</b>	<b>xxvii</b>
<b>Chapter 1. Introduction</b>	<b>1</b>
1.1 Introduction . . . . .	2
1.2 Visual motion detection by the fly visual system . . . . .	3
1.3 Yaw response and flight control steering muscles . . . . .	6
1.4 Receptive field organisation of insect neurons . . . . .	7
1.5 Models of motion detection . . . . .	8
1.6 Velocity estimation in insects . . . . .	12
1.7 Thesis overview . . . . .	13
1.8 Original contributions . . . . .	15
<b>Chapter 2. Velocity Estimation Using The Template Model</b>	<b>17</b>
2.1 The Template Model . . . . .	18
2.2 Prototyping Platform . . . . .	19
2.3 Colour Templates . . . . .	20

2.4	Pre-Template Filtering . . . . .	21
2.4.1	Spatial Averaging . . . . .	21
2.4.2	Multiplicative Noise Cancelation . . . . .	22
2.4.3	Experimental Results . . . . .	23
2.5	Post Template Filtering . . . . .	24
2.5.1	Windowing Operation . . . . .	24
2.5.2	Template Pairs . . . . .	26
2.5.3	Experimental Results . . . . .	26
2.6	De-noising the Colour Templates . . . . .	28
2.7	Measuring Angular Velocity . . . . .	29
2.8	Conclusions . . . . .	36
<b>Chapter 3. Reichardt Correlator Model</b>		<b>39</b>
3.1	A Simple Reichardt Correlator . . . . .	40
3.2	Correlator response to broadband images . . . . .	41
3.3	Dror's Elaborated Reichardt Correlator . . . . .	42
3.4	Experimental Verification . . . . .	45
3.5	Conclusion . . . . .	53
<b>Chapter 4. Comparison of the Template and the Reichardt models</b>		<b>55</b>
4.1	Comparison of Reichardt correlator vs Template model . . . . .	56
4.1.1	Template model response . . . . .	56
4.2	Conclusion . . . . .	59
<b>Chapter 5. Contrast adaptation</b>		<b>61</b>
5.1	Elaborated Reichardt Correlator with contrast adaptation . . . . .	62
5.2	The Insect Visual System . . . . .	62
5.2.1	Retina . . . . .	62
5.2.2	Lamina . . . . .	63
5.2.3	Medulla . . . . .	63
5.2.4	Lobula . . . . .	64
5.3	Natural stimuli . . . . .	64

5.4	Elaborated motion detector model . . . . .	66
5.5	Motion adaptation in the fly visual system . . . . .	69
5.6	Contrast adaptation . . . . .	70
5.7	Experimental Verification . . . . .	70
5.8	Contrast Gain Reduction — Feedback Adaptive EMD model . . . . .	71
5.9	Conclusion and future work . . . . .	73
<b>Chapter 6. Pattern noise</b>		<b>77</b>
6.1	Pattern noise . . . . .	78
6.2	Presence of Pattern Noise . . . . .	79
6.2.1	Electrophysiology methods . . . . .	79
6.2.2	Electrophysiology results . . . . .	79
6.2.3	Modelling results . . . . .	80
6.3	Receptive Field Shape and Pattern Noise . . . . .	81
6.3.1	Total Sample Of All EMDs . . . . .	82
6.3.2	Square Lattice . . . . .	82
6.3.3	Randomly Sampled Array . . . . .	82
6.3.4	Circular Sampled Array . . . . .	82
6.4	Sampling Results . . . . .	83
6.5	Role of Natural Image Statistics . . . . .	84
6.6	Conclusion . . . . .	85
<b>Chapter 7. Effect of Saturation on Pattern noise</b>		<b>95</b>
7.1	Saturation or Compressive non-linearity . . . . .	96
7.2	Pattern Noise . . . . .	96
7.2.1	Pattern noise at different contrasts and different speeds . . . . .	96
7.2.2	Electrophysiological results . . . . .	96
7.2.3	Modelling results . . . . .	98
7.3	Effect of Saturation on pattern noise . . . . .	100
7.3.1	Saturation at the correlator input . . . . .	100
7.3.2	Saturation at the correlator arms . . . . .	101

7.3.3 Saturation at the output . . . . . 101

7.4 Effect of Saturation on Contrast dependance . . . . . 102

7.4.1 Saturation at more than one points in the model . . . . . 103

7.5 Conclusion . . . . . 103

**Chapter 8. Effect of non-linearity on the performance of the elaborated model 119**

8.1 Relative error . . . . . 120

8.2 Role of additional components . . . . . 120

8.2.1 Spatial pre-filtering . . . . . 120

8.2.2 Temporal pre-filtering . . . . . 121

8.2.3 Output Integration . . . . . 122

8.3 Elaborated EMD model with adaptation . . . . . 122

8.3.1 Saturation . . . . . 124

8.3.2 Saturation at the correlator input . . . . . 124

8.3.3 Saturation at the correlator arms . . . . . 125

8.4 EMD model with adaptation and saturation . . . . . 126

8.4.1 Coefficient of Variation . . . . . 129

8.5 Conclusion . . . . . 131

**Chapter 9. Pattern noise study on different image structures 135**

9.1 Response of Fly HS Neurons to Naturalistic Images . . . . . 136

9.1.1 Evidence of Pattern Noise—Electrophysiology Results . . . . . 136

9.1.2 Evidence of Pattern Noise—Modelling Results . . . . . 139

9.2 Implementation of Saturation . . . . . 139

9.3 Images with Disrupted Vertical Contours . . . . . 142

9.4 Pattern Noise Analysis Using Different Images . . . . . 145

9.5 Conclusion . . . . . 151

**Chapter 10. Modelling a yaw sensor using our elaborated model 157**

10.1 A 16 pixel yaw sensor . . . . . 158

10.2 Conclusion . . . . . 160

<b>Chapter 11. Conclusion</b>	<b>163</b>
11.1 Introduction . . . . .	164
11.2 Thesis Summary . . . . .	164
11.2.1 Horridge Template Model . . . . .	164
11.2.2 Reichardt model . . . . .	165
11.2.3 Pattern noise . . . . .	165
11.3 Future Work . . . . .	166
11.4 Horridge model . . . . .	166
11.5 Reichardt model . . . . .	166
11.5.1 Pattern Noise . . . . .	167
11.6 Summary of original contributions . . . . .	167
11.7 In closing . . . . .	168
<b>Appendix A. Testing of the template model using Vision Egg software</b>	<b>169</b>
A.1 Vision Egg . . . . .	169
A.2 Measuring angular velocity . . . . .	169
A.2.1 Using a rotating drum . . . . .	170
A.2.2 Using Vision Egg software . . . . .	170
A.2.3 Analysis of Results . . . . .	178
A.3 Experiment to compare Template model response with Reichardt correlator response using Vision Egg . . . . .	179
A.4 Conclusion . . . . .	183
<b>Bibliography</b>	<b>185</b>
<b>Glossary</b>	<b>197</b>
<b>Resume</b>	<b>199</b>
<b>Scientific Genealogy</b>	<b>201</b>





# Abstract

Although motion processing in insects has been extensively studied for over almost 40 years, velocity detection in insects and how the insect brain computes the velocity of a moving feature, independent of its size or contrast, is a major enigma that remains unsolved. This study examines the accuracy of velocity estimation using two biologically inspired models of motion detection, (i) the Horridge template model and (ii) the Reichardt correlator model. Various extensions and enhancements of these models are implemented with the goal of achieving robust velocity measurements.

The template model is one of the prominent models of motion detection, which was proposed by Horridge in 1990. This Thesis further extends this model with the aim of improving accuracy in velocity detection using chrominance as well as luminance channels with various error checking mechanisms using different stimuli. Then the template model response is compared with Dror's elaborated Reichardt model and electro-physiological experimental results obtained from the fly visual system using similar stimuli in each case. A modified Reichardt model is shown to give a more similar response to that of fly neurons.

In order to improve velocity performance of the Reichardt model, it is necessary to reduce contrast dependence of the correlator response as well as to make it independent of the structure of the visual stimuli. With this aim, the Reichardt model is then further elaborated to include contrast adaptation by a feedback adaptive mechanism and a clear reduction in contrast dependency is demonstrated. The deviation of the correlator response depending on the stimulus is termed as pattern noise. To reduce this pattern noise, the Reichardt correlator model is further extended to implement compressive non-linearity or saturation. It is seen that saturation has a profound effect on the shape of the pattern noise. Further studies on pattern noise is then performed in this Thesis using different stimuli at different speeds and contrasts. Work carried out in this Thesis on the affect of various receptive field shapes on the pattern noise reveals circular sampled arrays reduce pattern noise and hence, based on this result, a small 16 pixel yaw sensor using our elaborated model is built that shows promising performance with various potential applications.



# Statement of Originality

This work contains no material that has been accepted for the award of any other degree or diploma in any university or other tertiary institution and, to the best of my knowledge and belief, contains no material previously published or written by another person, except where due reference has been made in the text.

I give consent to this copy of the thesis, when deposited in the University Library, being available in all forms of media, now or hereafter known.

---

Signed

---

Date



# Acknowledgments

This PhD has been a very stimulating and a memorable experience and there are many people whom I have to thank for it. First and foremost I thank my supervisors for all their support and encouragement throughout out my course.

I will always be grateful to my supervisor Prof Derek Abbott for introducing me to the field of insect vision and for inspiring me to take up this Ph.D inspite of the various doubts and concerns I had. I thank him for his valuable ideas and guidance with the template model research and for encouraging me to write papers and attend conferences, which has helped me a lot.

I take this opportunity to express my immense gratitude to my supervisor Prof David O' Carroll for being a constant source of inspiration through out the tenure of my PhD. I extend my sincere thanks for his continuous support and guidance with the Reichardt correlator modelling and for helping me to understand insect neurology and electrophysiological experiments.

I thank my colleagues Dr Tamath Rainsford and Dr Andrew Straw for their physiological data and Dr Mark McDonnell, Dr Karin Nordstrom, Leonard Hall, Gretel Png, Eng-Leng Mah and Matthew Berrymann for making this a fun experience. Many thanks to Rado Guzinski, Khao Nguyen, and Zi H. Yong for their vision egg experimental data.

I gratefully acknowledge the funding provided by the United States Air Force Office of Scientific Research/Asian Office for Aerospace Research and Development, United States Air Force Research Laboratory, The Sir Ross and Sir Keith Smith Fund and the Australian Research Council. I would also like to thank the Cooperative Research Center for Sensor Signal and Information processing (CSSIP) for their top-up scholarship. Special thanks are also due to the staff of the School of Electrical and Electronic Engineering especially the computer support staff and the academic and general staff for their generous help.

I will forever stay indebted to my parents for their love and faith in me, my dad—for teaching me to believe in me, my mom—for being there always for me and my sister Sreeshma—for lightening things up.

## Acknowledgments

---

Finally, I owe everlasting gratitude to my dear husband Raj for being an epitome of love, support and patience and for helping me in every possible way and my five year old daughter Riya for being my inspiration and for always giving me a reason to smile.

– Sreeja Rajesh.

# Thesis Conventions

**Typesetting.** This Thesis is typeset using the LaTeX 2e software. Processed plots and images were generated using Matlab 6.1 (Mathworks Inc.). Adobe Illustrator 10 was used to produce schematic diagrams and other drawings. Vision EGG software (<http://www.visionegg.org>) was used to generate stimuli for electrophysiological experiments.

**Spelling.** Australian English spelling has been adopted throughout, as defined by the Macquarie English Dictionary (A. Delbridge, Ed., Macquarie Library, North Ryde, NSW, Australia, 2001). Where more than one spelling variant is permitted such as biassing or biasing and infra-red or infrared, the option with the fewest characters has been chosen.

**Referencing.** The Harvard style is used for referencing and citation in this Thesis.





# Publications

- SREEJA RAJESH, TAMATH RAINSFORD, RUSSELL BRINKWORTH, DEREK ABBOTT AND DAVID O'CARROLL (2007). Implementation of saturation for modelling pattern noise using naturalistic stimuli, *Proceedings of SPIE on BioMEMS and Nanotechnology II*, **6414**, Art. No. 641424.
- SREEJA RAJESH, DAVID O'CARROLL AND DEREK ABBOTT (2006). A 16 pixel yaw sensor for velocity estimation, *Proceedings of SPIE on BioMEMS and Nanotechnology II*, **6036**, Art. No. 603618.
- RADO GUZINSKI, KHAO NGUYEN, ZI YONG, SREEJA RAJESH, DAVID O'CARROLL AND DEREK ABBOTT (2006). Characterization of insect vision based collision avoidance models using a video camera, *Proceedings of SPIE on Biomedical Applications of Micro- and Nanoengineering II*, **6036**, Art. No. 60361D.
- SREEJA RAJESH, DAVID O'CARROLL AND DEREK ABBOTT (2005). Man-made velocity estimators based on insect vision, *Smart Materials and Structures*, **14**, p. 413—424.
- SREEJA RAJESH, TAMATH RAINSFORD, DAVID O'CARROLL AND DEREK ABBOTT (2005). Modeling pattern noise in responses of fly motion detectors to naturalistic scenes, *Proceedings of SPIE on Biomedical Applications of Micro- and Nanoengineering II*, **5651**, p. 160—173.
- SREEJA RAJESH, ANDREW STRAW, DAVID O'CARROLL AND DEREK ABBOTT (2005). Effect of spatial sampling on pattern noise in insect-based motion detection, *Proceedings of SPIE on Smart Structures, Devices, and Systems II*, **5649**, p. 811—825.
- SREEJA RAJESH, ANDREW STRAW, DAVID O'CARROLL AND DEREK ABBOTT (2005). Effects of compressive non linearity on insect based motion detection, *Proceedings of SPIE on Smart Structures, Devices, and Systems II*, **5649**, p. 798—810.
- ANDREW BUDIMIR, SEAN CORRELL, SREEJA RAJESH AND DEREK ABBOTT (2004). Implementation of insect vision based motion detection models using a video camera, *Proceedings of SPIE on Smart Structures, Devices, and Systems II*, **5649**, p. 596—606.

- SREEJA RAJESH, DAVID O'CARROLL AND DEREK ABBOTT (2004). Effects of nonlinear elaborations on the performance of a Reichardt correlator, *Proceedings of SPIE on BioMEMS and Nanotechnology*, **5279**, p. 287—303.
- SREEJA RAJESH, DAVID O'CARROLL AND DEREK ABBOTT (2003). Velocity estimation and comparison of two insect-vision-based motion-detection models, *Proceedings of SPIE on Smart Materials, Structures, and Systems*, **5062**, p. 401—412.
- SREEJA RAJESH, DAVID O'CARROLL AND DEREK ABBOTT (2002). Elaborated Reichardt correlators for velocity estimation tasks, *Proceedings of SPIE on Biomedical Applications of Micro- and Nanoengineering*, **4937**, p. 241—253.
- HUNG NGUYEN, SREEJA RAJESH AND DEREK ABBOTT (2001). Motion detection algorithms using template model, *Proceedings of SPIE on Electronics and Structures for MEMS II*, **5279**, p. 78—90.

# List of Figures

Figure		Page
1.1	Visual system of insects . . . . .	5
<hr/>		
2.1	Directionally motion sensitive templates . . . . .	19
2.2	Nomenclature for photoreceptor channel input intensities . . . . .	21
2.3	Diagram illustrating the source of the multiplicative noise . . . . .	23
2.4	Example templates with no pre-filtering . . . . .	24
2.5	Example templates with spatial averaging . . . . .	25
2.6	Example templates with MNC pre-filtering . . . . .	25
2.7	Applying the windowing algorithm to the templates . . . . .	27
2.8	Applying the template pair algorithm to the output . . . . .	27
2.9	Colour templates before denoising . . . . .	28
2.10	Colour templates after de-noising. . . . .	29
2.11	Template response (dark object in front of light background) . . . . .	30
2.12	Comparison of angular velocity curves with no pre-filtering . . . . .	31
2.13	Comparison of angular velocity curves with spatial averaging . . . . .	32
2.14	Comparison of angular velocity curves with MNC filtering . . . . .	32
2.15	Comparison of angular velocity curves with template pair filtering . . . . .	33
2.16	Comparison of angular velocity curves with windowing method . . . . .	33
2.17	Comparison of angular velocity curves with averaging and template pair method . . . . .	34
2.18	Comparison of angular velocity curves with averaging and windowing method	34
2.19	Comparison of angular velocity curves with MNC and template pair technique	35
2.20	Comparison of angular velocity curves with MNC and windowing method .	35
<hr/>		
3.1	The Reichardt correlator has two receptors . . . . .	41

## List of Figures

---

3.2	Block diagram of an elaborated correlator model . . . . .	43
3.3	Mean horizontal power spectra of random textures used in experiments . .	47
3.4	Velocity response curves for a model correlator for random texture images of various densities, as predicted from the power spectra . . . . .	48
3.5	Velocity response curves measured at six different texture densities for a single HSNE neuron . . . . .	49
3.6	Optimum velocity as a function of texture density for several neurons . . .	50
3.7	Spatial and temporal frequency tuning for the HSNE neuron of Fig. 3.5 . .	51
3.8	Velocity response curves measured for the same HSNE cell at different contrasts . . . . .	52
<hr/>		
4.1	Velocity response curves measured at six different texture densities for the Template model . . . . .	57
4.2	Benchmark angular velocity measured by the tachometer versus benchmark velocity measured using the Template model . . . . .	58
<hr/>		
5.1	The elaborated EMD array . . . . .	65
5.2	The panoramic natural image given as stimulus to the EMD model . . . . .	66
5.3	Spatially low pass filtered naturalistic image used as stimuli . . . . .	67
5.4	Space time matrix obtained when a single row of EMDs is simulated at a constant velocity . . . . .	67
5.5	The input and the output responses of a single EMD from the modelled array moving with constant velocity of $200^\circ/s$ . . . . .	68
5.6	(A) To test motion adapted responses, the velocity is increased step-wise, with interleaved bursts of adapting motion (constant speed). The velocity is increased in steps with time, (B) The mean correlator response of the EMD array model to a natural image moving with velocity increasing in steps across the EMD array . . . . .	68
5.7	Block diagram of a feed back adaptive EMD model . . . . .	72
5.8	The input and the output responses of one EMD from the adaptive EMD array in response to the test sequence illustrated in Figure 5.6 . . . . .	73

---

---

5.9	The correlator response of an un-adaptive EMD array at three different contrasts . . . . .	74
5.10	The correlator response of an adaptive EMD array at three different contrasts	75

---

6.1	Presence of pattern noise in the response of a fly neuron with the image presented moving at high velocity . . . . .	87
6.2	Presence of pattern noise in the response of a fly neuron with the image presented moving at low velocity . . . . .	88
6.3	Presence of pattern noise in the simulated response of our elaborated model with the image presented moving at high velocity . . . . .	89
6.4	Presence of pattern noise in the simulated response of our elaborated model with the image presented moving at low velocity . . . . .	90
6.5	The panoramic images used as stimuli to our model . . . . .	91
6.6	Total EMD array . . . . .	91
6.7	Rectangular EMD sample . . . . .	92
6.8	Random EMD sample . . . . .	92
6.9	Row or circular EMD sample . . . . .	92
6.10	Error bars and responses obtained from the simulation of a rectangular, random, row and total array of EMDs . . . . .	93
6.11	Simulated mean correlator response for square, circular, random and total array of EMDs . . . . .	94
6.12	The relative errors obtained from the simulation of the square, random, circular and total array of the EMDs . . . . .	94

---

7.1	The panoramic natural image given as stimulus to the EMD model . . . . .	97
7.2	Pattern noise in fly response for images moving at high and low speeds at a low contrast of 0.2 . . . . .	105
7.3	Pattern noise in fly response for images moving at high and low speeds at a high contrast of 1 . . . . .	106
7.4	Pattern noise in simulation result for images at high speed at a low contrast of 0.2 . . . . .	107

---

## List of Figures

---

7.5	Pattern noise in simulation result for images at low speed at a low contrast of 0.2 . . . . .	108
7.6	Pattern noise in simulation result for images at high speed at a high contrast of 1 . . . . .	109
7.7	Pattern noise in simulation result for images at low speed at a high contrast of 1 . . . . .	110
7.8	Simulated phase aligned results with saturation implemented only at the input . . . . .	111
7.9	Simulated phase aligned results with saturation implemented only at the correlator arms . . . . .	112
7.10	Simulated phase aligned result with saturation implemented only at the output . . . . .	113
7.11	Comparison of simulated phase aligned results with saturation implemented at the input, arms and at the output . . . . .	114
7.12	Simulated mean correlator response at three different contrasts with saturation implemented only at the input . . . . .	115
7.13	Simulated mean correlator response at three different contrasts with saturation implemented only at the correlator arms . . . . .	115
7.14	Simulated mean correlator response at three different contrasts with saturation implemented only at the output . . . . .	116
7.15	Simulated mean correlator response at three different contrasts with saturation implemented at more than one point in the model . . . . .	117
<hr/>		
8.1	The panoramic natural images given as stimulus to the EMD model . . . . .	121
8.2	Comparison of simulated relative error with contrast adaptation and without contrast adaptation . . . . .	123
8.3	Simulated mean relative error of our elaborated EMD model . . . . .	124
8.4	Simulated mean correlator response with saturation implemented at the photoreceptors at three different contrasts . . . . .	125
8.5	Simulated mean relative error of the elaborated EMD model with adaptation and saturation at the input . . . . .	126
8.6	Simulated mean correlator response at three different contrast with saturation implemented at the input and arms . . . . .	127

---

8.7	Comparison of simulated mean correlator response with saturation included at the input with that of the model with saturation implemented at the input and arms . . . . .	127
8.8	Block diagram of an elaborated EMD model including feedback adaptation and saturation . . . . .	128
8.9	The variation of feedback signal ( $S_{fb}$ ) as the correlator output is increased is shown here . . . . .	128
8.10	Simulated mean relative error of the total elaborated model . . . . .	130
8.11	Simulated cumulative sum of mean correlator responses of the total elaborated model for a large set of images. . . . .	131
8.12	The bar graph showing the mean response with error bars before the adaptation stage and after adaptation. . . . .	132
8.13	The bar graph showing the coefficient of variation before adaptation and after adaptation of the elaborated model . . . . .	132
<hr/>		
9.1	The panoramic natural images given as stimulus to the EMD model . . . .	137
9.2	Electrophysiological experimental set up . . . . .	138
9.3	Comparison of physiological and modelling results using the same stimulus at different phases and their phase aligned and time aligned responses . . .	140
9.4	Phase aligned simulation results obtained by running the model at $180^\circ/s$ using the image 1 shown in Figure 9.1 at a contrast of 1 . . . . .	142
9.5	Phase aligned simulation results obtained from the elaborated model with saturation implemented at the correlator arms and at the output, superimposed on the physiological data . . . . .	143
9.6	The three images of Figure 9.1 with their vertical contours disrupted. . . .	144
9.7	Phase aligned simulation results obtained by running the model at 180 degrees per sec using the disrupted image 1 . . . . .	145
9.8	Phase aligned simulation results obtained from the elaborated model with saturation implemented at the correlator arms and at the output, superimposed on the physiological data using disrupted image 1 . . . . .	146
9.9	Comparison of physiological pattern noise of the original and disrupted images . . . . .	147

---

## List of Figures

---

9.10	Comparison of simulated pattern noise of the original and disrupted images	152
9.11	Simulated phase aligned results superimposed with the physiological phase aligned fly response using Image 1 . . . . .	153
9.12	Simulated phase aligned results superimposed with the physiological phase aligned fly response using Image 2 . . . . .	154
9.13	Simulated phase aligned results superimposed with the physiological phase aligned fly response using Image 3 . . . . .	155
<hr/>		
10.1	Panoramic images given as stimuli . . . . .	158
10.2	Test speeds with interleaved bursts of adapting speeds . . . . .	159
10.3	Mean correlator response with and without saturation . . . . .	160
10.4	Mean correlator response of three rows of EMDs . . . . .	160
10.5	Velocity response of the small yaw sensor . . . . .	161
<hr/>		
A.1	Comparison of angular velocity curves with no pre-filtering using the rotating drum . . . . .	171
A.2	Comparison of angular velocity curves with no pre-filtering using the Vision Egg software . . . . .	172
A.3	Comparison of angular velocity curves with spatial averaging using the rotating drum . . . . .	172
A.4	Comparison of angular velocity curves with spatial averaging using the Vision Egg software . . . . .	173
A.5	Comparison of angular velocity curves with MNC filtering using the rotating drum . . . . .	173
A.6	Comparison of angular velocity curves with MNC filtering using the Vision Egg software . . . . .	174
A.7	Comparison of angular velocity curves with template pair filtering using the rotating drum . . . . .	174
A.8	Comparison of angular velocity curves with template pair filtering using the Vision Egg software . . . . .	175
A.9	Comparison of angular velocity curves with averaging and template pair method . . . . .	175



A.10 Comparison of angular velocity curves with the averaging and template pair method using the Vision Egg software . . . . . 176

A.11 Comparison of angular velocity curves with MNC and template pair technique 176

A.12 Comparison of angular velocity curves with MNC and template pair technique 177

A.13 Comparison of angular velocity curves with windowing method . . . . . 177

A.14 Velocity response curves measured at five different texture densities with the Horridge template model using Vision Egg stimuli . . . . . 180

A.15 Normalized velocity response curves measured at five different texture densities using the Horridge template model . . . . . 182

A.16 Benchmark angular velocity presented by the vision egg experiment versus angular velocity determined by insect vision system . . . . . 183



# List of Tables

Table		Page
9.1	Cross covariance values for each model . . . . .	148
9.2	Relative error values for each model . . . . .	149
9.3	Cross correlation values obtained by correlating the first half of the image on the second half . . . . .	150
9.4	Relative error and cross covariance values at different window size . . . . .	150